ADVANCED FUNCTIONAL MATERIALS
www.afm-journal.de

Nature's Guard: UV Filter from Pollen

*Chungmo Yang, Abdul Rahim Ferhan, Heeseon Yang, Nanum Chung, Mohammed Shahrudin Ibrahim, Young Hwan Choe, Jingyu Deng, Jung Ryeol Lee, and Nam-Joon Cho**

Protection against ultraviolet (UV) radiation has long safeguarded humans against skin diseases. However, recent studies have uncovered that the UV-filtering compounds in sunscreens can have harmful effects on marine ecosystems. This discovery has led to a major re-evaluation and reformulation of the chemicals used in UV filter. Even with the ban on several of these compounds, current sunscreens on the market still contain other harmful substances. To reverse the adverse effects currently afflicting the ecosystem and provide a genuinely sustainable solution, inspiration is drew from nature to develop a plant-derived, pollen microgel UV filter. The in vitro and in vivo investigations showed that the microgel exhibited excellent ultraviolet B (UVB) protection to the skin with no toxic effects. More importantly, the introduction of the microgels to simulated seawater showed that it supports long-term healthy survival of corals, with minimal heat accumulation in the applied formulation, which is vital for maintaining the delicate balance in the marine ecosystem. It is anticipated that these promising results will spark a paradigm shift toward sustainable UV protection strategies that not only protect humans but also remedy the natural ecosystem.

1. Introduction

Imagine standing on the shoreline, where the warmth of the sun meets the cool ocean breeze. Just as a diver plunges into the depths of the sea to uncover hidden wonders, scientists delve into the mysteries of nature, striving to understand the intricate balance that sustains life on Earth. Unfortunately, human activities, particularly the use of sunscreens containing harmful ultraviolet (UV)-filtering chemicals, have disrupted this delicate balance, with coral reefs—some of the most vibrant ecosystems on the planet—facing the severe consequence.

The natural ecosystem consists of a diverse array of interconnected ecologies that operate synergistically to maintain a delicate balance of biological, chemical, and physical processes.[1] Such balance is crucial for sustaining environmental stability, maintaining biodiversity, and supporting the complex interactions between species and their habitats.[2] Hence, any form of ecological disruption is systemic and can have detrimental effects on the overall ecosystem. In light of global warming, climate change, and the plastic pandemic,[3] the threat to coral ecologies posed by toxic UV-filtering compounds released to the sea in the order of several thousand tons potentially aggravates the degradation of marine and terrestrial ecologies alike.[4] Such disruptions can adversely affect biodiversity and compromise the well-being of all living organisms, including humans.

Estimates from environmental monitoring studies and global market analyses suggest that several thousand tons of UV-filtering compounds are introduced into aquatic environments annually via both direct and indirect pathways.[5] Direct input occurs through the wash-off of sunscreen during recreational water activities such as swimming and snorkeling, with studies indicating that up to 25% of applied sunscreen can be released into seawater within 20 min of exposure.[6] Indirect contributions arise from domestic wastewater effluent, which receives residues from routine personal care product use (e.g., moisturizers, lip balms, and cosmetics), as well as from industrial sources, including plastics and surface coatings, where UV absorbers are commonly added. These residues are often only partially removed during wastewater treatment and subsequently discharged into surface waters.[7]

Cumulatively, these sources contribute to the pervasive presence of UV-filtering compounds such as oxybenzone and octocrylene in marine environments, where they have been detected at concentrations exceeding ecotoxicological thresholds. Global sunscreen sales exceed 500,000 metric tons annually, and

C. Yang, A. R. Ferhan, M. S. Ibrahim, Y. H. Choe, J. Deng, N.-J. Cho
School of Materials Science and Engineering
Nanyang Technological University
50 Nanyang Avenue, Singapore 639798, Singapore
E-mail: njcho@ntu.edu.sg
C. Yang, A. R. Ferhan, M. S. Ibrahim, Y. H. Choe, J. Deng, N.-J. Cho
Centre for Cross Economy
Nanyang Technological University
60 Nanyang Avenue, Singapore 637551, Singapore
H. Yang, N. Chung, J. R. Lee
Department of Translational Medicine
Seoul National University College of Medicine
Seoul 08826, Republic of Korea
H. Yang, N. Chung, J. R. Lee
Department of Obstetrics and Gynecology
Seoul National University Bundang Hospital
Seongnam 13620, Republic of Korea

The ORCID identification number(s) for the author(s) of this article can be found under https://doi.org/10.1002/adfm.202516936

DOI: 10.1002/adfm.202516936

conservative environmental release estimates 5,000–10,000 tons of UV-filtering compounds may enter aquatic systems each year, assuming 5–10% rate of wash-off or discharge.[8] While this quantity does not uniformly impact all marine ecosystems, accumulation is most pronounced in shallow, semi-enclosed coastal zones with limited water exchange, high tourism activity, and elevated solar UV indices.

Environmental monitoring has identified UV filter hotspots in sensitive marine ecosystems including the Caribbean, the Mediterranean, and island tourist attractions across Southeast Asia. In these regions, seasonal peaks in UV filter concentrations often coincide with tourist influxes, raising the likelihood of acute and chronic exposure for coral communities. Measured concentrations of oxybenzone in reef waters during peak tourism have reached or exceeded 1,000 ng L^{-1}, surpassing thresholds known to cause coral larval deformities and bleaching.[9] Such localized accumulations pose a significant ecological burden, particularly to coral reefs already under stress from climate change and other anthropogenic pressures. These patterns underscore the need for a holistic understanding of UV filter sources, transport mechanisms, and spatiotemporal accumulation dynamics to guide effective mitigation strategies and sustainable product development.

Over the years, scientists, regulators, and industry players have played their roles in seeking a viable solution. Recently, Vuckovic et al. revealed how oxybenzone-based sunscreens, especially when combined with other environmental stressors, may significantly contribute to the declining health of coral populations.[10] Along this line, oxybenzone and a series of other toxic compounds have been banned across the industry, and sunscreens are currently produced containing compounds that are deemed toxic-free.[9] Additionally, some coastal communities have banned the use of sunscreens containing specific UV filters that are considered harmful to corals.[5,11] Nevertheless, growing scientific consensus has highlighted the environmental risks posed by widely used synthetic UV filters such as oxybenzone, octinoxate, and octocrylene, which remain common in commercial formulations.[12] These compounds have been detected in coastal waters at ecologically relevant concentrations and are linked to coral bleaching, impaired larval development, oxidative stress, endocrine disruption, and bioaccumulation in marine organisms.[13] In response, multiple governments and regulatory agencies, particularly in environmentally sensitive and tourism-dependent regions, have moved to restrict or formally ban the use of these filters,[14] underscoring the urgent need for safer, environmentally sustainable alternatives.[15]

Although various plant-derived compounds and biodegradable carriers have been explored as environmentally friendly alternatives to synthetic UV filters, many of these systems rely on photolabile active ingredients such as flavonoids or polyphenols, which often require synthetic stabilizers, encapsulation systems, or chemical modification to enhance photostability and efficacy.[16] Such formulation complexities not only diminish the overall ecological benefit but also introduce additional barriers to scalability, regulatory acceptance, and cost-effectiveness. These limitations underscore the need for intrinsically photostable, biocompatible materials that can deliver effective UV protection with minimal formulation burden. Aiming for a solution that is both good for people and better for the environment, we turned to nature for inspiration. Observing how certain living systems have successfully survived extreme environmental stressors, such as climate change, UV radiation, and ozone depletion, over centuries, we focused on strategies adopted by plants to safeguard their genetic material. Our investigation revealed that plant pollen, with its multilayered structure, offers both physical and chemical protection against environmental hazards. Building on this natural model, we have established methods to develop a range of plant-derived materials through a series of transformations converting hard pollen into soft matter, leading to the production of microgel, paper, and sponges.[17] In the context of UV protection, the microencapsulated gel holds significant promise as a topical coating. Our findings demonstrate that this coating provides effective UV light protection while exhibiting non-toxicity, high biocompatibility, and environmental safety. Crucially, our findings indicate that this approach is benign to marine ecosystems, including coral reefs, offering a promising avenue for sun protection that aligns with the delicate ecological balance of nature (**Figure 1**).

2. Results and Discussion

2.1. UV-Shielding Properties of Natural Pollen and Its Derivatives

Pollen plays a critical role in ensuring plant survival and the success of reproduction by offering robust protection to genetic materials against harsh UV radiation from the sun.[18] This is attributed to its exine layer composed of sporopollenin,[19] which contains antioxidative and UV-absorbing phenolic compounds such as p-coumaric acid and ferulic acid.[20] Intriguingly, a recent report provided evidence that these compounds were produced in abundance by pollen grains in response to an increase in ultraviolet B (UVB) intensity during the late Permian period mass extinction event, allowing them to survive the extremely intense radiation.[21] On this basis, we were motivated to develop a novel class of sustainable UV-shielding materials derived from natural pollen, beginning with the development of a pollen-based UV filter (**Figure 2A**). Given that the process involves transforming natural pollen (NP) into defatted pollen (DFP) and sporopollenin exine capsules (SEC) before obtaining a microgel form suitable for use as a UV filter coating, it is crucial to first confirm that the UV-shielding properties are preserved throughout the series of chemical treatments developed by our group.[22] In our demonstration, we mainly employed Camellia pollen due to its abundance and processability and included Sunflower pollen.[23] While morphological changes were clearly observed for both pollen species when NP was converted to DFP and SEC (Figure S1A, Supporting Information), the UV–vis absorbance spectra showed similar profiles, with maximum absorbance in the UV range, which gradually decreases to reach a minimum of zero absorbance in the red region of the visible wavelength range. In fact, with each treatment from NP to SEC, the pollen acquired the ability to absorb more light over a longer wavelength range close to the UV region (Figure S1B,C, Supporting Information).

We then investigated the effects of ultraviolet A (UVA) and UVB irradiation on cell death and proliferation of human keratinocytes (HaCaT cells), in the presence of pollen particles with optimized concentration, which ensures uniform coverage (Figure S2, Supporting Information). Upon 2.5 min of UVA

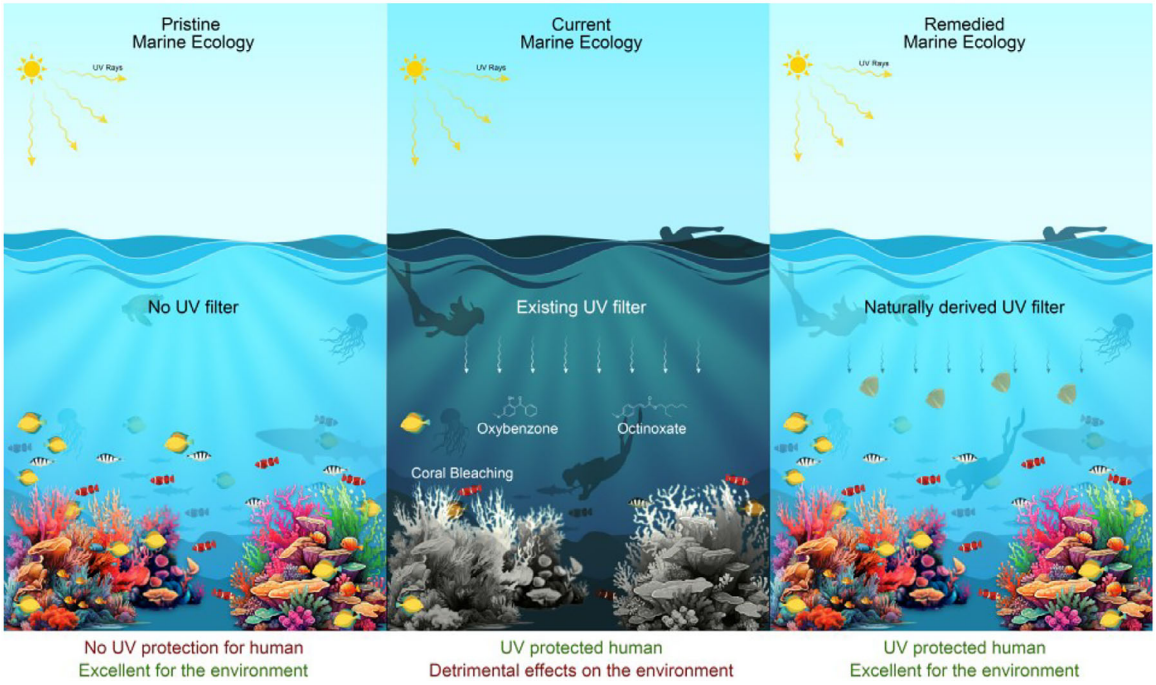

Figure 1. Visual representation of various states of the marine ecology. The marine ecology in its pristine state without contamination from any form of leeched ultraviolet (UV) filters (left), in the current state with contamination from presently available UV filters that are detrimental to the ecology (middle), and the anticipated remedied state in the presence of next-generation naturally derived UV filters (right). Image Credit: Batika Saxena.

irradiation, cell viability decreased to 60.09% (±3.54%) when measured immediately after exposure. It continued to decrease with longer exposure time down to 34.69% (±2.24%) for the case of 10-min exposure, however, UVA irradiated cells proliferated up to 88.13% (±3.89%) after 48 h of culture (Figure S3A–C, Supporting Information). On the other hand, cell viability remained above 77.74%, even for the case of 10-min exposure, strongly suggesting the effectiveness of pollen particles in blocking UVA (Figure S3D, Supporting Information). The quantifications were further corroborated through direct visual observation of the HaCaT cells and LIVE/DEAD staining, which shows that majority of cells remained viable 48 hrs post-exposure (Figure S3E,F, Supporting Information). In contrast, UVB irradiation inhibits cell proliferation and induces cell cycle arrest and apoptosis, partially mediated by p53 through p21.[24] In our results, after 10 min of exposure, cell viability measured immediately was 54.33% (±3.38%) (Figure S4A, Supporting Information). However, it reduced to 10.05% (±1.85%) when measured 48 h after exposure (Figure S4B,C, Supporting Information). When pollen particles blocked UVB, cell viability remained above 99% even after 10 min of UVB irradiation (Figure S4D–F, Supporting Information).

In addition, we also checked the effectiveness of NP, DFP, and SEC to shield UV irradiation by measuring the levels of reactive oxygen species (ROS), since UV irradiation is known to induce apoptosis by producing ROS. In the absence of pollen particles, the irradiation of UVA and UVB to HaCaT cells increased ROS production by a factor of 4.47 and 2.46, respectively, compared to the control group (i.e., without any irradiation). However, upon shielding by pollen particles (i.e., NP, DFP, and SEC), UVA and UVB irradiation increased ROS production by only a factor 1.67 and 1.38 on average, respectively. This provides further evidence that pollen particles, even after treatment, maintains the UV-shielding capability, resulting in the suppression of ROS production (Figure S5, Supporting Information).

2.2. In Vitro Evaluation of Pollen Microgel as a UV Filter

Following confirmation that the UV-shielding properties of pollen particles were retained throughout the transformation from NP to SEC, we then proceeded to convert the hard pollen particles into soft pollen microgel, which can be uniformly coated on various surfaces for a range of UV filter applications in practical settings. This is achieved through a mild alkaline treatment[22] resulting in a suspension of pliable pollen particulates (i.e., pollen microgel) in polar solvent (Figure 2B). Interestingly, UV–vis absorbance measurements revealed that even in the microgel form, the pollen sample exhibited a similar absorbance profile to the SEC (Figure 2C), with Camellia pollen microgel displaying stronger UVB absorption compared to Sunflower pollen microgel (Figure S6A, Supporting Information). We then performed LIVE/DEAD and ROS assays, which showed that the introduction of pollen microgels to HaCaT cells resulted in higher cell viability and lower ROS production compared to the no-protection group upon exposure to UVA and UVB for more than 10 min (Figure 2D; Figure S6B–E, Supporting Information).

Chemical analysis using pyrolysis gas chromatography-mass spectrometry (GC/MS) revealed for the first time the presence of UV-absorbing phenolic coumaric acid and ferulic acid in pollen microgel (Figure S7A,B, Supporting Information). This indicates that although the exine of the pollen was softened during the microgel synthesis process, the chemical makeup of the

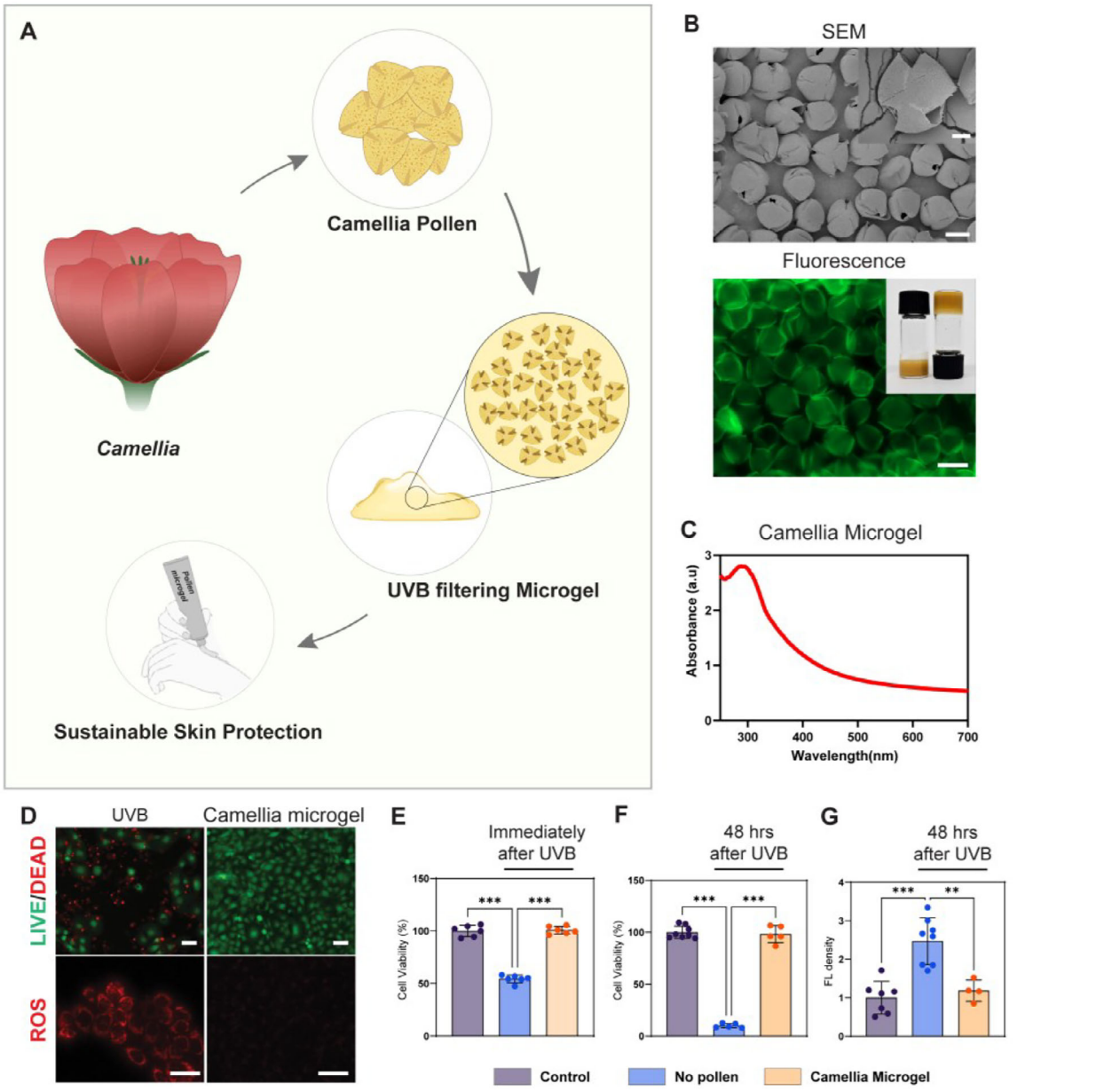

Figure 2. Development and efficacy of pollen-based sunscreen. A) Schematic illustration of the process of creating pollen-based sunscreen: pollen is harvested from Camellia, processed into a microgel, and then used in sunscreen formulations for sustainable skin protection. B) (top) SEM images of Camellia pollen microgel. Scale bar = 20 µm (10 µm, inserted image) (bottom) image of auto-fluorescence microscope of Camellia pollen microgel and inverted tube testing. Scale bar = 50 µm C) UV–vis absorbance (a.u.) spectrum of Camellia microgel D) LIVE/DEAD and ROS assays showing cell viability and barely produced ROS reactive oxygen species production after 10min UVB irradiation protected with Camellia microgel. Scale bars = 100 µm. Quantitative analysis of cell viability. E) immediately after UVB exposure, F) 48 h after UVB exposure, and G) ROS production under different conditions: Control, no pollen (UV only), and protected with Camellia microgel (*$p < 0.05$, **$p < 0.01$, ***$p < 0.001$).

sporopollenin (i.e., of the microgel) remains largely consistent with that of native sporopollenin, with both coumaric acid and ferulic acid retaining their UV-absorbing properties. On a broader context, this implies that with careful modulation of the synthesis process, the native characteristics of pollen can be retained even when new properties are introduced during the transformation to microgel. Most importantly, this proves that pollen microgels can effectively serve as a UV-shielding material.

Quantitative analyses revealed that immediately after UVB irradiation for 10 min, cell viability of 100.78% (±3.30%) was achieved in the presence of Camellia microgel, which was comparable to the control group (i.e., without irradiation) (Figure 2E). In contrast, in the absence of pollen microgel, UVB irradiation decreased the cell viability to 10.05% (±1.85%). Remarkably, a high cell viability of 98.21% (±7.26%) was maintained in the presence of Camellia microgel, even after 48 h of UVB irradiation

(Figure 2F). Subsequently, the quantification of ROS production after 48 h of UVB irradiation revealed only a slight increase by a factor of 1.32 (±0.36) in the presence of Camellia microgel, as opposed to more than two-fold increase without microgel protection (Figure 2G). After the irradiation of UVB for 30 min, the cell viability after 48 h reached ≈5% in the no-protection group. However, it remained above 65% blocked UV by the pollen microgels. Taken together, these results further corroborate that the UV-shielding effect is maintained even after gelation, confirming the promise of pollen microgels as UV filters.

2.3. In Vivo Cytotoxicity Evaluation of Pollen Microgel Using ICR Mouse Model of UV-Induced Skin Damage

The exposure to UV radiation is well-known to cause skin diseases and various skin abnormalities.[25] To assess the degree of UV protection to the skin that can be offered by topical treatment of pollen microgel and evaluate any potential cytotoxicity, we employed the ICR mouse model and triggered UV-induced skin damage by means of UVB irradiation (312 nm) with an intensity of 1.6 mW cm^{-2} for 13 min once every 24 h over three consecutive days. Histological examination of skin biopsy specimens conducted using hematoxylin and eosin (H&E) staining after the three-day period revealed the loss of epidermis and significant hemorrhaging in untreated skin sections exposed to UVB irradiation compared to normal skin (i.e., without exposure to UVB) (**Figure** 3A; Figure S8A–C, Supporting Information). In contrast, sections that were topically applied with Camellia and Sunflower microgel successfully preserved the epidermis. Epidermal thickness measurements revealed significant thinning of the epidermis from 30.41 µm (±8.57 µm) in normal skin without UV exposure to 9.59 µm (±3.35 µm) after UVB irradiation (Figure 3B). However, there was no significant change in epidermal thickness for protected skin sections post-irradiation, with final thicknesses of 28.59 µm (±9.43 µm), 31.12 µm (±9.56 µm), and 33.42 µm (±8.59 µm) for sections topically applied with commercial sunscreen, Camellia microgel, and Sunflower microgel, respectively (Figure 3B; Figure S8D,E, Supporting Information). Along this line, further analysis using Masson's Trichrome (MT) staining revealed that the application of pollen microgel preserved the collagen structure within the dermis, which appears largely blue (i.e., MT positive), corresponding to regions of well-organized and intact collagen fibers (Figure 3B; Figure S8F, Supporting Information). Conversely, the skin section without protection appears uniformly red, corresponding to denatured collagen throughout the dermis. Quantitative analyses of MT staining revealed a significant decrease in MT positive area, which corresponds to the loss of collagen structure, from 40.8% (±9.21%) in normal skin without UV exposure to 16% (±3.28%) after UVB irradiation. On the other hand, MT positive areas of 46% (±5.36%), 46.80% (±10.28%), and 48.40% (±6.34%) were recorded post-irradiation for sections applied with commercial sunscreen, Camellia microgel, and Sunflower microgel, respectively (Figure 3C; Figure S8G, Supporting Information).

Furthermore, histological examination using Toluidine Blue staining revealed that the application of Camellia and Sunflower microgel did not result in the reduction of mast cells, as observed in the unprotected sections (Figure S8H, Supporting Information). Since mast cells are resident cells in the epidermis for rapid activation in the event of skin damage,[26] the reduction of these cells implies that the healing process in unprotected sections will be compromised. In other words, our results show that the protection with microgel prevented any form of intracellular damage within the dermis, which would have originated from UV ray penetration, while at the same time preserving the healing properties of the skin.[27] Taken together, these qualitative observations provide preliminary indications that pollen microgel are highly effective UV filters that offer similar, if not superior skin protection performance than conventional sunscreens even under intense UV radiation. Likewise, while the number of mast cells reduced drastically to 42.13% for unprotected sections (14.88 cells, ±4.62), no signification difference was observed between normal skin (35.33 cells, ±11.05), and those protected with commercial sunscreen (37.44 cells, ±8.15), Camellia microgel (35.5 cells, ±6.61) and Sunflower microgel (35.44 cells, ±10.52) (Figure S8I, Supporting Information).

We then analyzed immune responses in the cutaneous tissue by measuring changes in gene expression related to fibrosis and inflammation following UVB irradiation. Considering that UVB irradiation adversely affects the expression of Col1a1, Col3a1, TGF-b, Fn-1, IL-1b, TNF-a, and IL-6 genes, which collectively influence various molecular pathways involved in inflammation, extracellular matrix (ECM) remodeling, and cell signaling,[28] we measured the mRNA expression of these pro-fibrotic and pro-inflammatory genes post-irradiation. We observed a significant upregulation of gene expression in the unprotected sample, particularly for Col1a1, Col3a1, IL-1b, and IL-6 (Figure 3D–H). Specifically, the detected Col1a1 and Col3a1 mRNA levels in unprotected samples were up to 10- and 24-fold higher than in normal unexposed samples. Across all these genes, the protection with commercial screen and pollen microgel successfully suppressed upregulation, except for a slight increase in Col1a1 mRNA levels in the case of protection with commercial sunscreen (Figure S9, Supporting Information).

Subsequently, we quantified the expression of Fn-1, Collagen 1, αSMA, CTGF, Pro-iL1b, IL-1b, and TNF-a by Western blotting across both unprotected and protected samples and analyzed the results through a heat map and protein expression level measurements (Figure 3I–K; Figure S10, Supporting Information). In unprotected samples, UV irradiation led to an increased expression of Fn-1 and Collagen 1 by a factor of 4.97 (±0.15) and 5.21 (±0.78), respectively, indicating the occurrence of tissue repair and maintenance of ECM remodeling.[29] While a slight increase by a factor of 1.44 (±0.03) was observed for the actin αSMA, there was a dramatic rise by a factor of 14.33 (±1.42) for the growth factor CTGF, signifying fibroblast activation and fibrosis.[30] At the same time, significantly elevated expression of cytokines Pro-IL1b, IL-1b, and TNF-a reflects inflammation and immune response,[29] collectively highlighting damage control and healing of the cutaneous tissue. Specifically, Pro-IL1b, IL-1b, and TNF-a increased by factors of 18.58 (±4.31), 15.01 (±3.41), and 2.38 (±0.59), respectively. Remarkably, the topical application of Camellia and Sunflower microgels prevented increased expressions of these ECM proteins, growth factors, and cytokines, confirming their efficacy in protecting against UV-induced fibrosis and inflammation. No significant difference was observed compared to samples protected by commercial

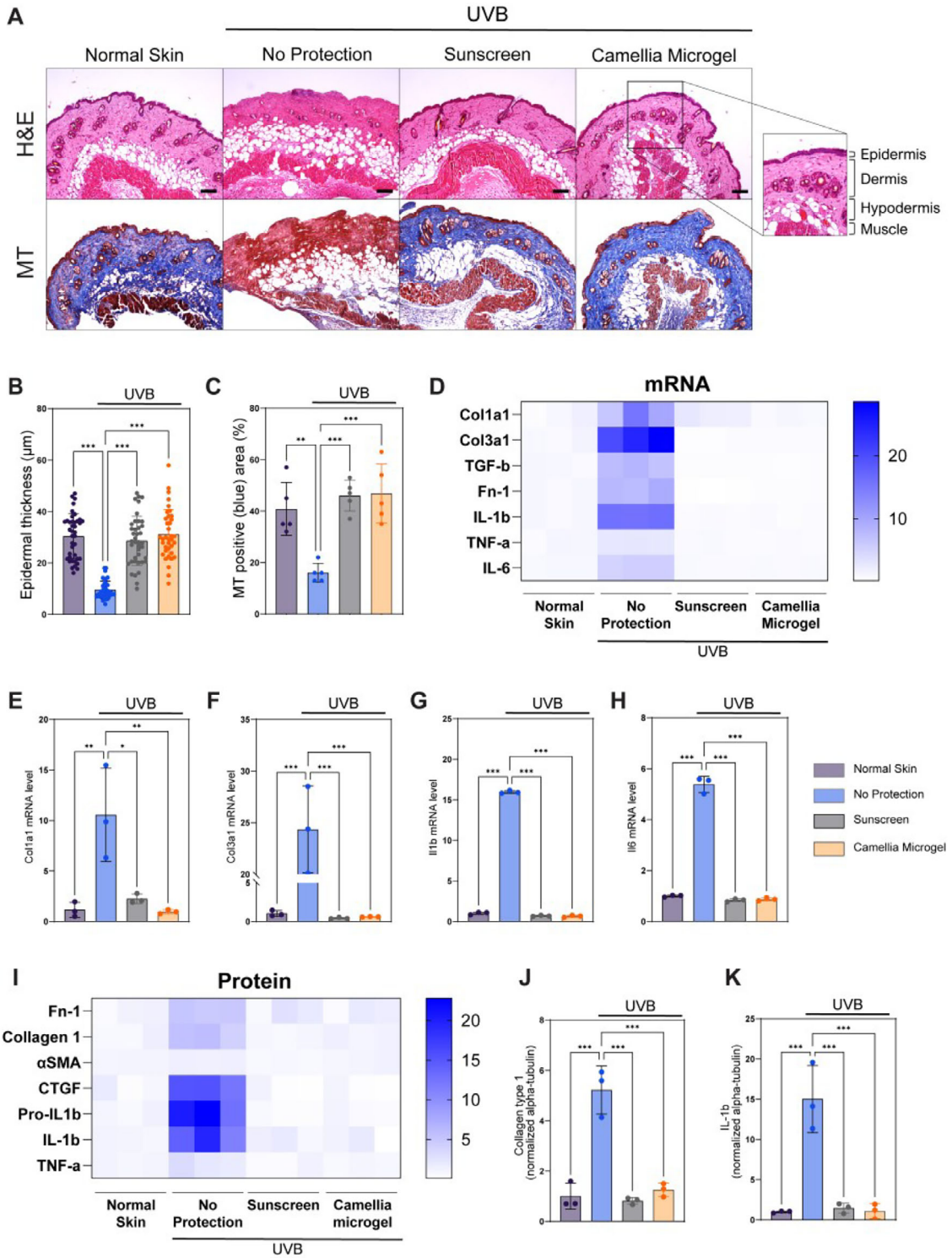

Figure 3. In vivo assessment of pollen-based sunscreen on UV-induced skin damage. A) Histological sections of skin stained with Hematoxylin and Eosin (H&E) and Masson's Trichrome (MT) under different conditions: Normal Skin, UV irradiation: No Protection, Sunscreen, and Camellia Microgel. Scale bar: 100 μm. B,C) Quantification of epidermal thickness and MT positive area (%) of the skin sections after UVB irradiation under different conditions. D) Heatmap of relative mRNA expression levels of genes (Col1a1, Col3a1, TGF-β, Fn-1, IL-1β, TNF-α, and IL-6) across different treatments. E–H) mRNA expression levels of (E) Col1a1, (F) Col3a1, (G) IL-1β, and (H) IL-6 in Normal Skin, UV irradiation: No Protection, Sunscreen, and Camellia Microgel. I) Heatmap of relative protein levels of markers (Fn-1, Collagen 1, αSMA, CTGF, pro-IL1β, IL-1β, TNF-α) across different treatments. J–M) Protein expression levels of (J) Collagen 1 and (K) IL1β in Normal Skin, UV irradiation: No Protection, Sunscreen, and Camellia Microgel. *$p < 0.05$, **$p < 0.01$, ***$p < 0.001$.

sunscreen. These findings collectively underscore the dual protective action of pollen microgels, which not only prevent biophysical damage as evidenced by histological staining,[31] but also by not triggering immune responses through the mitigation of inflammatory cytokines, avoiding any cytotoxic effects. This comprehensive protection confirms the potential of pollen microgels as highly effective non-toxic UV filters that offer substantial defense against both immediate and long-term UV-induced damage.

2.4. Evaluation of the Potential Impact of Pollen Microgel UV Filter to the Natural Ecosystem

Considering the adverse effects of commercial sunscreen on the natural environment,[32] there is a pressing need to develop eco-friendly solutions that are not only beneficial for consumers but also help address the ongoing imbalance of the natural ecosystem. Following this line, our results advocate for further development and application of pollen microgels as topical sunscreens, providing a foundation for protective formulations that safeguard human skin health in environments with high UV exposure. Within this context, a universal parameter widely used by general consumers for measuring protection against UVB radiation is the Sun Protection Factor (SPF). It indicates the effectiveness of sunscreen products in preventing damage to the skin, suppressing premature aging, and reducing the risk of skin cancer.[33] To evaluate the performance of our pollen microgel UV filters as next-generation consumer-grade sunscreens, the in vitro SPF levels were calculated using the Mansur method.[34] Typically, sunscreens with SPF levels above 30 are necessary for extended outdoor activities.[35] While Sunflower microgels achieved in vitro SPF close to 5, Camellia microgels achieved SPF 27.31 (±4.72) comparable to commercial sunscreen 29.38 (±0.91) at the same concentration with no cytotoxicity (Figure S11, Supporting Information), which makes it ideal for activities under intense sun exposure, most popularly at the beach and out at sea. In relation to this, while many sunscreens have been marketed as 'reef-safe' or 'coral-friendly', the veracity of these claims remains questionable.[15,36] For example, although some products are labelled 'oxybenzone-free', they still contain traces of UV filter compounds that are considered potentially harmful to the human hormonal system as well as marine life, including coral reefs.[37]

Since the marine ecosystem represents a vital component within the interconnected network of the overall natural ecosystem of our planet, which could potentially mediate the effects of global warming and climate change,[38] we first assessed the ability of our pollen microgel UV filters to preserve marine life when applied as sunscreens. We cultured *Acropora sp*. in simulated seawater under different conditions, including the introduction of commercial sunscreen labelled as 'oxybenzone-free' as well as our pollen microgels. To better mimic natural marine environments, each coral exposure tank was equipped with a submersible water pump operating to ensure continuous water circulation throughout the experiment. This setup provided a moderate, quasi-dynamic flow (≈13 times turnover per hour), which promoted homogeneous dispersal of test substances while minimizing mechanical stress on the corals. *Acropora sp*. is a genus of coral within the *Acroporidae* family and was selected as a representative coral since they play an important role in reef-building and contribute to the formation of the coral reef framework while providing habitat and shelter for a wide range of marine organisms, including fish, invertebrates, and other reef-dwelling species.[6b] Over a 14-day period, the *Acropora sp*. cultured in simulated seawater introduced with Camellia and Sunflower microgels retained its color as per the blank control (**Figure** 4A,B; Figure S12A and Videos S1–S3, Supporting Information). In contrast, the coral cultured in commercial sunscreen was bleached on day 2, indicating that the coral tissues were under stress resulting from the loss of symbiotic algae,[39] and became completely white on day 14 (Figure 4A,B), consistent with previous studies.[40] Besides, the corals cultured in both Camellia and Sunflower microgels, remained healthy and retained its color even after 30 days and 60 days, similar to the blank control (Figure S12B, Supporting Information). This confirms that the pollen microgels exhibit no toxicological effects to marine systems. Given their hollow, highly hydrated structure and estimated bulk density close to that of seawater, the pollen microgels are expected to exhibit near-neutral buoyancy, enabling prolonged suspension and dispersion under typical marine flow conditions with minimal sedimentation similar to hydrogels.[41] Their composition, comprising naturally derived biopolymers and a UV-resilient sporopollenin shell, suggests a favorable environmental profile, with gradual biodegradation via microbial and oxidative pathways and resistance to photofragmentation. Compared to conventional synthetic UV filters, which often persist in marine systems, these microgels offer enhanced ecological compatibility and a reduced risk of long-term accumulation.

We then compared the thermal regulatory effects of our camellia pollen microgels against commercial sunscreen when directly exposed to sunlight (Figure 4C). Understanding thermal effects is important not only within the context of topical application to skin but also since sunscreens that are released during water-based activities can potentially alter the heat capacity of sea water, which can in turn adversely affect the delicate balance in the overall natural ecosystem. Our measurements reveal that the temperature of the skin surface topically applied with commercial sunscreen rose rapidly from 30 °C to ≈37 °C under direct sunlight within 20 min (Figure 4D,E). However, with topical application of Camellia microgel, the temperature gradually increased to ≈33 °C after 20 mins, consistently remaining 5 °C lower than the bare skin surface (Figure 4D,E). Furthermore, we evenly spread the same volume of commercial sunscreen and pollen microgel on glass slides and subjected them to direct UV lamp exposure to detect thermal regulation effects (Figure S13A, Supporting Information). The temperature of commercial sunscreen increased relatively quickly, reaching ≈25 °C after 10 min. In comparison, the temperature of pollen microgel maintained a lower temperature and increased to ≈25 °C over an extended period of 30 min (Figure S13B,C, Supporting Information). These results indicate that the pollen microgels mitigate the rapid rise in skin temperature and provided prolonged thermal protection against UVB irradiation.

The observed reduction in surface temperature for pollen microgel-treated skin during simulated sunlight exposure is primarily attributed to the spectral optical properties of the microgel, particularly its reduced absorbance in the visible to NIR range (i.e., 400–900 nm). This spectral window accounts for the

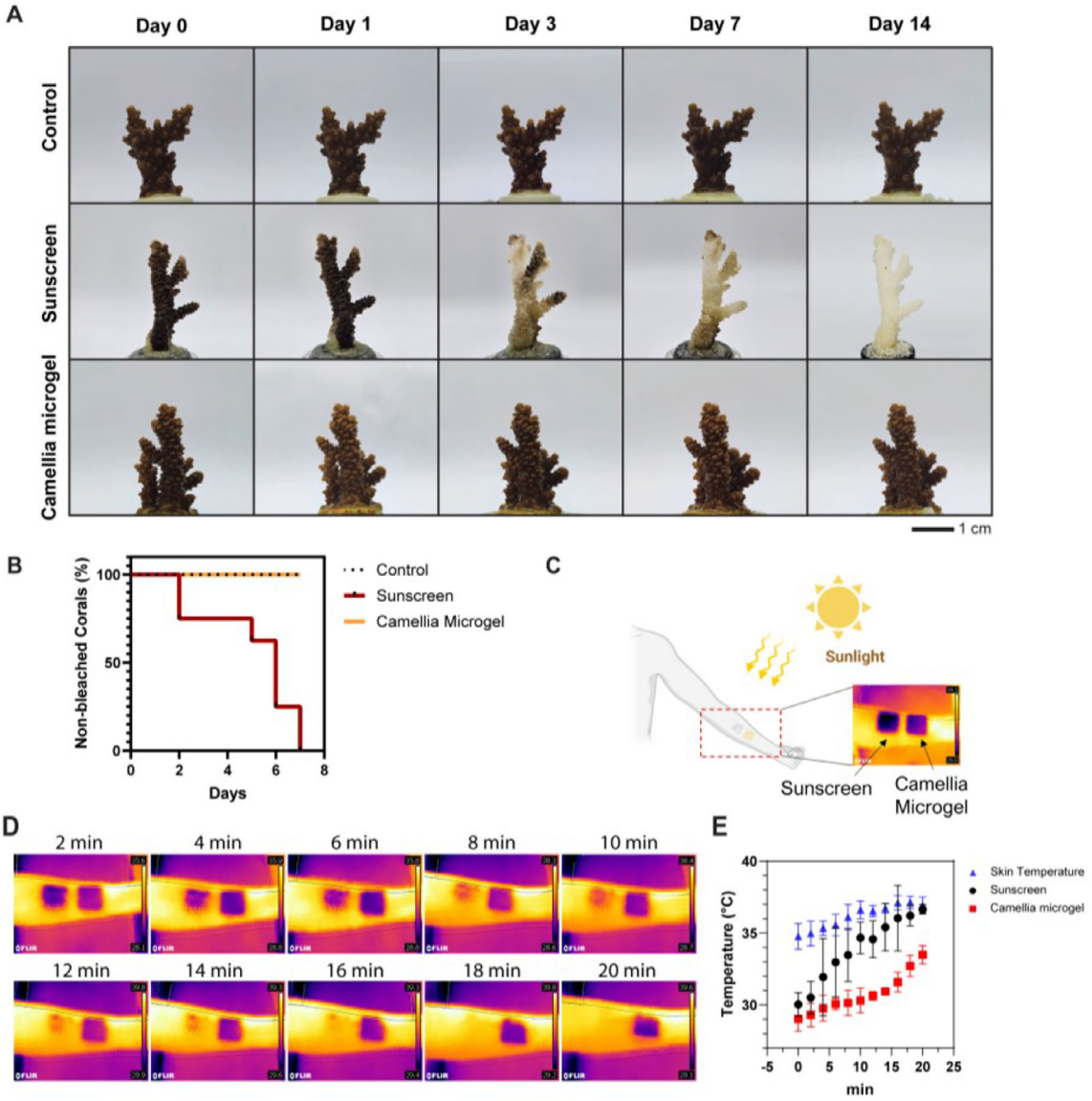

Figure 4. Evaluation of pollen-based sunscreen properties on coral bleaching and skin surface temperature. A) Photographs showing coral bleaching over 14 days under different treatments: control (seawater), commercial sunscreen (chemical), and Camellia microgel. Scale bar = 1 cm. B) Survival curve depicting the percentage of non-bleached corals over time when treated with control (seawater, $n = 4$), commercial sunscreen ($n = 8$), and Camellia microgel ($n = 4$). C) Schematic illustration of the experimental setup for measuring surface temperature under sunlight exposure. The comparison is made between commercial sunscreen and Camellia microgel. D) Thermal images captured at 2-min intervals up to 20 min, showing temperature changes on surfaces treated with commercial sunscreen and Camellia microgel. E) Recorded skin temperature (°C) over time under sunlight exposure. Measurements were recorded for a control untreated area, as well as areas treated with commercial sunscreen and Camellia microgel.

majority of solar thermal energy, and materials with strong absorbance in this region typically undergo greater photothermal conversion, resulting in elevated surface temperatures. In contrast, the pollen microgel exhibits high absorbance in the ultraviolet (UV) range (i.e., <400 nm) but significantly attenuated absorbance across the visible to NIR range, as observed in Figure 2C and Figure S1 (Supporting Information). As a result, the amount of incident solar energy converted into heat is markedly lower for the microgel-coated surface relative to the commercial sunscreen film. This inherently limits localized thermal energy accumulation and contributes to the lower steady-state surface temperature observed via infrared thermography. Importantly, the thermal regulation effect is not driven by bulk heat capacity or thermal mass of the hydrated film, which would primarily influence transient heat conduction rather than equilibrium surface temperature under continuous irradiation. Instead, the cooling behavior is dominated by the ability of the microgel to selectively filter out thermally active wavelengths of solar radiation, thereby reducing net photothermal input and subsequent surface heating.

Altogether, the positive outcomes from our in vitro and in vivo studies, as well as in simulated practical setting, collectively

affirm the effectiveness of our pollen microgel as a non-toxic UV filter, which can be safely applied for topical protection of the human skin without any adverse effects to marine life and the natural ecosystem. The pollen microgel platform offers a holistic approach to environmental sustainability, demonstrating eco-compatibility not only in its end-use application but also throughout its preparation process. The synthesis is based on mild, aqueous-phase chemistry that avoids the use of harsh organic solvents, synthetic cross-linkers, or energy-intensive conditions. All chemical inputs are used at low concentrations, and reaction byproducts can be safely neutralized by means of standard wastewater treatment protocols. The primary raw material (i.e., Camellia pollen) is a renewable and agriculturally abundant resource, commonly collected from otherwise discarded or surplus floral biomass. This not only minimizes waste but also establishes a sustainable resource base for scalable materials development and mass production. Along this line, it is also worth noting that since the widespread bleaching of corals can in fact be reversed through regaining the symbiotic algae with the removal of environmental stressors,[39] which in this case is in the form of toxic compounds. Hence, the timely adoption of pollen microgel as a UV filter in sunscreens provides the opportunity for coral ecosystems to recover over time, potentially reinstating the natural balance across different ecologies.

3. Conclusion

In summary, the conversion of natural plant components with inherent protective properties into engineered materials that protect other aspects of the environment represents an innovative approach. This concept can be extended across various applications to mitigate the adverse effects that have impacted our natural ecosystems.[42] As demonstrated in this work, pollen microgel serves as an excellent candidate for use in biomedical and cosmetics applications, especially considering its outstanding performance in protecting cells from UVA and UVB radiation. Since it is devoid of allergic materials following the defatting processes, it is well-poised to serve as a sustainable UV filter. This not only opens new avenues for skin protection formulations but also contributes significantly to environmental remedy efforts by potentially reversing the negative ecological impact of sunscreen on marine life. Beyond the development of pollen microgel-based skin protection formulations, the concept of utilizing natural protective properties of plant-derived materials for protecting other natural elements can be adopted to develop other types of protective films and biocoatings that can be applied onto a wide range of surfaces, such as fruits and vegetables, which could potentially safeguard or revive other ecologies as well.

4. Experimental Section

Defatting of Bee Pollen: The defatting process of Camellia bee pollen (Camellia sinensis L) followed the established protocols from previous reports.[17,22] Initially, bee pollen was mixed with deionized water and agitated continuously for 2 h at 50 °C. After removing large contaminants through a 200 µm nylon mesh, water was removed through vacuum filtration. The resulting pollen particles were treated with acetone for 3 h and washed at room temperature. Following ambient drying overnight, the dried pollen was dispersed in diethyl ether under continuous stirring conditions for 2 h at room temperature twice, followed by washing and the removal of diethyl ether by vacuum filtration. To finalize the defatting process, the remaining pollen was mixed with fresh diethyl ether overnight with stirring. The resulting pollen was vacuum-filtrated and air-dried in the fume hood. The defatted pollen was stored in the desiccator until use.

Preparation of Pollen Microgels: To fabricate pollen microgels, the defatted pollen was treated with KOH using procedures from previous works.[17,22] Initially, the defatted pollen was stirred in a 10% KOH solution and refluxed for 2 h at 80 °C in a PTFE-coated round bottom flask. The resulting mixture was filtered through a 35 µm nylon mesh and washed with fresh KOH solution until the filtrate cleared. The remaining pollen was mixed with fresh KOH solution and incubated for 24 h. After incubation, the pollen suspension was filtered through a 35 µm nylon mesh and washed with deionized water until the pH was 7.5. The final products were collected and stored at 4 °C until use.

Fundamental Characterizations of Pollen Particles: The UV absorbance spectra of pollen samples (i.e., natural pollen, sporopollenin, defatted pollen, and pollen microgels) were measured between 250–700 nm using a microplate reader (Tecan SPARK, Tecan, Männedorf, Switzerland). The morphology of Camellia pollen microgels was characterized using a field-emission scanning electron microscope (FESEM) (JSM-7600F Schottkyfield-emission scanning electron microscope). The fluorescence image of Camellia pollen microgels were taken with Zeiss Axio Observer Z1 microscope (Carl Zeiss, Oberkochen, Germany).

To cover the surface using pollen particles, the concentration of natural pollen, defatted pollen, and sporopollenin in 96-well plates (100 µl solution added to each well) was optimized. The particles (0.078, 0.156, 0.312, 0.625, 1.25, 2.5, and 5 mg ml^{-1}) sank to the bottom of the well after a few minutes. Fluorescence microscopic images were then taken, followed by image analysis of the particle-covered area. The covered area increased with higher concentrations of pollen particles. The sporopollenin exhibited a slightly higher covered area at the same concentrations compared to the other particles. At 625 µg ml^{-1}, the area covered by sporopollenin reached ≈30%, and at 1250 µg ml^{-1}, it reached 50%. In contrast, the defatted pollen covered ≈20% at 625 µg ml^{-1} and 65% at 2500 µg ml^{-1}, while natural pollen covered 30% at 1250 µg ml^{-1} and 55% at 2500 µg ml^{-1}. All types of pollen particles covered above 95% of the surface area at 5000 µg ml^{-1}. The results demonstrated that sporopollenin had a higher covered area than other particles, which could be attributed to it being lighter than natural or defatted pollen by extraction processes, leading to more particles per unit weight. Additionally, since defatted pollen was produced by removing contents from natural pollen particles, it exhibited a larger covered area than natural pollen. Based on this, the concentrations of sporopollenin, defatted pollen, and natural pollen were fixed at 5 mg ml^{-1} (100 µl) in subsequent experiments to achieve particle surface coverage of at least 95%.

Cell Culture: Immortalized HaCaT keratinocytes were obtained from Cell Lines Service GmbH (Eppelheim, Germany). Cells were maintained in DMEM (Life Technologies, Inc., Grand Island, NY, USA) supplemented with 10% fetal bovine serum (FBS, Gibco, NY, USA), 100 U ml^{-1} penicillin-streptomycin (Sigma Aldrich, St. Louis, MO, USA). Medium was refreshed every three days.

In Vitro Evaluation of UV Protection Properties of Pollen Particles and Microgels: The cell viability test was then performed to evaluate the protective effects of pollen particles against UV irradiation. The cells were plated with 10,000 cells per well in 96-well plates and allowed to settle for 24 h before the experiment. After the cells adhered, pollen particles (natural pollen, sporopollenin, and defatted pollen) were added at concentrations corresponding to the well coverage (5 mg ml^{-1}). The cells were then exposed to UV radiation in a UV chamber (ELC-500, Electro-lite Corp, USA) for 2.5, 5, 7.5, 10, and 20 min for both UVA (15 mW cm^{-2}) and UVB (1.6 mW cm^{-2}). The pollen particles were then removed by rinsing the wells with PBS. Cell viability was measured by using the Cell Counting Kit-8 (Dojindo, Japan) immediately and 48 h after UV irradiation. Fluorescent staining was performed using the LIVE/DEAD assay kit (Invitrogen, Carlsbad, CA, USA) to visualize cell viability. The cell viability test was carried out for the pollen microgel using a similar method, with UVA or UVB irradiation

times of 10, 20, and 30 min after doping with microgel on plate lids. Cell viability was measured by using the Cell Counting Kit-8 (Dojindo, Japan) at 0, 24, and 48 h after UV irradiation. Fluorescent staining was performed using the LIVE/DEAD assay kit (Invitrogen, Carlsbad, CA, USA) to visualize cell viability.

In Vitro Reactive Oxygen Species (ROS) Quantification: The amount of ROS was determined by CellROX Deep Red Oxidative Stress Reagent (Invitrogen, Carlsbad, CA, USA) at 0 and 48 h after UVA and UVB irradiation as described by the manufacturer. Briefly, cell culture and UV irradiation procedures followed the description above. The medium was treated with CellROX Deep Red Oxidative Stress Reagent at a final concentration of 5 µM and incubated at 37°C for 30 min, followed by three washes with DPBS. To confirm the qualitative evaluation of intracellular ROS distribution, the labeled cells were confirmed using a microplate reader (Tecan SPARK, Tecan, Männedorf, Switzerland) and Zeiss Axio Observer Z1 microscope (Carl Zeiss, Oberkochen, Germany).

In Vitro Sun Protection Factor (SPF) Calculation: The in vitro SPF number was determined according to the spectrophotometric method described by Mansur' method.[34] The absorbance of commercial sunscreen and pollen microgels (i.e., Sunflower and Camellia), were recorded between 290–320 nm using a UV–vis Spectrophotometer (UV-2700, Shimadzu, Japan). The SPF levels were calculated using the following equation:

$$SPF_{in\ vitro} = CF \times \sum_{290}^{320} EE\,(\lambda) \times I\,(\lambda) \times Abs\,(\lambda) \quad (1)$$

where EE (λ): erythemal effect spectrum; I (λ): solar intensity spectrum; Abs (λ): absorbance of sunscreen product; CF: correction factor (= 10).

In Vivo Evaluation of UV-Induced Skin Damage: All animal experimental procedures in this study were conducted in accordance with the approval of the Institutional Animal Care and Use Committee (IACUC) at Seoul National University Bundang Hospital (Approval number: BA-2405-391-004-01). To assess the damage caused by UV radiation on the skin, an experiment involving female ICR mice 7–8 weeks old ($n = 5$) was conducted. Mice were randomly divided into various groups, namely Normal Skin, UV irradiation: No Protection, Sunscreen, and Camellia Microgel. The commercial sunscreen used in this study was oxybenzone-free and composed of octinoxate, ethylhexyl triazone, diethylamino hydroxybenzoyl hexyl benzoate, bis-ethylhexyloxyphenol methoxyphenyl triazine as chemical UV filters. Following anesthesia and hair removal, the respective samples were applied to designated areas of the skin. Subsequently, the mice were exposed to UV radiation at 1.6 mW cm^{-2} for 13 min every 24 h for 3 days to establish a UV-induced skin burn model. Skin biopsies were obtained using an 8 mm skin punch, with samples either stored at −20°C for future analysis or fixed in 4% paraformaldehyde (PFA) for histological examination. The paraffin-embedded sections (4 µm thickness) were stained with haematoxylin & eosin, Masson's trichome, and Toluidine blue. The epidermal thickness and keratin area were quantified using the ImageJ software.

Total RNA was extracted using Trizol (Life Technologies, Gaithersburg, MD, USA) followed by the immediate cDNA synthesis from 2000 ng of extracted RNA using M-MLV Reverse Transcriptase kit (Promega, Madison, WA, USA). Quantitative real-time PCR was performed by amfiSure qGreen Q-PCR Master Mix (GenDEPOT, Katy, TX, USA) with ViiA 7 Real-Time PCR System (Applied Biosystems, Foster City, CA, USA). Data were normalized by housekeeping gene Gapdh as a control and quantitation of the fold change was determined by the comparative CT method. The information of primers used in this study is provided in Table S1 (Supporting Information).

The skin tissues were lysed in PRO-PREPTM Protein Extraction Solution (iNtRON Biotechnology, Sungnam, Republic of Korea) containing phosphatase inhibitors. Protein concentration was quantified with a BCA Protein Assay Kit (Thermo Scientific, Waltham, MA, USA) according to the manufacturer's instructions. Total protein (10 µg) was separated by SDS-PAGE and transferred onto PVDF membranes. The membranes were blocked in TBST with 5% skim milk or BSA for 45 min at RT and then immunoblotted with primary antibodies overnight at 4 °C. After washing in TBST, the blots were incubated with the HRP-conjugated secondary antibodies for 1 h at RT. The proteins were visualized by Immobilon Forte Western HRP Substrate (Merck Millipore, Burlington, MA, USA) in ChemidocTM MP Imaging System (Bio-Rad Laboratories, Hercules, CA, USA). Densitometric quantitation of protein bands was performed using ImageJ (National Institutes of Health, Bethesda, MD, USA).

Cytotoxicity of Commercial Sunscreen and Pollen Microgel: The cytotoxicity of commercial sunscreen and pollen microgel was evaluated using HaCaT cells cultured in DMEM (Life Technologies, Inc., Grand Island, NY, USA) supplemented with 10% FBS and 1% penicillin-streptomycin. Cells were seeded at 10,000 cells/well in 96 well-plates. The sunscreen was mixed with the culture medium to prepare a 10% (v/v) sunscreen-in-medium suspension. Pollen microgels were similarly prepared at 10% (v/v) in complete growth medium and added to the wells with serial dilution. After 24 h, the cell viability was assessed using the CCK-8 assay to quantify viable cells.

Coral Bleaching Test: To observe the coral bleaching caused by sunscreen ingredients or pollen microgels, an experiment was conducted by simulating the situation where sunscreen washes off into seawater. Coral bleaching occurs in almost all types of corals and is triggered by various factors, including elevated sea temperatures, ultraviolet exposure, pollution, and specifically, certain sunscreen ingredients such as oxybenzone, octocrylene, and octinoxate.[5,11] These chemicals could induce stress in corals, leading to the loss of their symbiotic algae, which causes the corals to bleach. In this study, *Acropora sp.* corals were selected because they are widely distributed in tropical and subtropical waters around the world, including the Indo-Pacific and the Caribbean. *Acropora sp.* corals, known for their diverse forms and rapid growth rates, play a crucial role in reef-building and were thus ideal for studying the general effects of sunscreen-induced bleaching. The *Acropora sp.* corals were obtained from a local aquarium (Haiyang & ReefMarketSG, Singapore). Corals were maintained in a recirculating artificial seawater system at 25 °C. Coral exposure experiments were conducted in 10 L simulated seawater tanks fitted with a submersible circulation pump delivering a consistent flow rate of 200 L h^{-1}. This setup maintained a continuous, gentle, low-shear current designed to mimic natural water movement in shallow reef environments, ensuring uniform dispersion of test substances without causing physical stress to the coral specimens throughout the exposure period. Photographic images were obtained on days 0, 1, 3, 5, 7, and 14 after commencing culture. For treatment, 1 ml of the sunscreen or pollen microgels was mixed with seawater and added to a 10 L seawater tank after a 24 h adaptation period. During culture, corals were monitored and counted once bleaching began. Images of the control and pollen microgel-treated groups were taken after 30 and 60 days.

Temperature Measurement and Thermal Imaging: To equalize the temperatures of the pollen microgel and sunscreen, they were left at room temperature for 2 h. Then,200 µl of each sample was applied in a square shape (3 cm x 3 cm) on two areas of the forearm. To ensure a fair and application-relevant comparison, the UV attenuation performance of the pollen microgels and commercial sunscreens was evaluated based on a standardized surface application dose (mg cm^{-2}), reflecting realistic usage conditions rather than the internal concentration of UV-active compounds. Temperature measurements and thermal imaging were conducted at 2-min intervals for 20 min under direct sunlight (between 2 and 3 PM in Singapore's average temperature and weather conditions). Sunscreen or pollen microgel (100 µL each) were spread on glass slides and continuously exposed to a UV lamp (365 nm, UVGL-58 handheld UV lamp) from a distance of 5 cm. During the 40-min exposure, temperature measurements and thermal imaging were conducted every 2 min. In both sets of experiments, temperature measurements were taken at four different points.

Statistical Analysis: All results are presented as the mean ±SD of independent experiments. The significance of statistical differences was analyzed using one-way ANOVA test (Prism 10; GraphPad Software, San Diego, CA, USA). $P < 0.05$ was regarded to have statistical significance.

Supporting Information

Supporting Information is available from the Wiley Online Library or from the author.

Acknowledgements

This research was supported by the Ministry of Education (MOE) in Singapore under the MOE AcRF Tier 3 grant (Grant No. MOE-MOET32022-0002) as well as the Korea Health Technology R&D Project through the Korea Health Industry Development Institute (KHIDI), funded by the Ministry of Health & Welfare, Republic of Korea (Grant No. HI22C1394) and Ministry of Agriculture, Food and Rural Affairs (Grant No. RS-2024-00403067). The research was also supported by the Korea Institute of Planning and Evaluation for Technology in Food, Agriculture, and Forestry (IPET) through a research collaboration agreement between RE:harvest Co., Ltd. and Nanyang Technological University (REQ0639147).

Conflict of Interest

The authors declare no conflict of interest.

Author Contributions

C.Y. and A.R.F. contributed equally to this work. N.J.C. conceptualized the study and was responsible for funding acquisition and project administration. The methodology was developed by C.Y., A.R.F., and N.J.C. The investigation was conducted by C.Y., A.R.F., J.D., H.Y., N.C., M.S.I., and J.R.L. Visualization of the data was performed by C.Y., J.D., and M.S.I. Supervision was provided by N.J.C. and J.R.L. The original draft of the manuscript was written by C.Y., A.R.F., and N.J.C., with review and editing contributions from C.Y., A.R.F., M.S.I., and N.J.C.

Data Availability Statement

The data that support the findings of this study are available on request from the corresponding author. The data are not publicly available due to privacy or ethical restrictions.

Keywords

environmentally friendly sunscreen, plant biomaterials, pollen microgel, ultraviolet filter

Received: July 7, 2025
Revised: July 22, 2025
Published online:

[1] G. B. Bonan, S. C. Doney, *Science* **2018**, *359*, aam8328.
[2] A. D. Barnosky, E. A. Hadly, P. Gonzalez, J. Head, P. D. Polly, A. M. Lawing, J. T. Eronen, D. D. Ackerly, K. Alex, E. Biber, J. Blois, J. Brashares, G. Ceballos, E. Davis, G. P. Dietl, R. Dirzo, H. Doremus, M. Fortelius, H. W. Greene, J. Hellmann, T. Hickler, S. T. Jackson, M. Kemp, P. L. Koch, C. Kremen, E. L. Lindsey, C. Looy, C. R. Marshall, C. Mendenhall, A. Mulch, et al., *Science* **2017**, 355.
[3] J. B. Lamb, B. L. Willis, E. A. Fiorenza, C. S. Couch, R. Howard, D. N. Rader, J. D. True, L. A. Kelly, A. Ahmad, J. Jompa, C. D. Harvell, *Science* **2018**, *359*, 460.
[4] J. Galamgam, N. Linou, E. Linos, *Lancet Planetary Health* **2018**, *2*, 465.
[5] a) C. L. Mitchelmore, E. E. Burns, A. Conway, A. Heyes, I. A. Davies, *Environ. Toxicol. Chem.* **2021**, *40*, 967; b) M. Moeller, S. Pawlowski, M. Petersen-Thiery, I. B. Miller, S. Nietzer, Y. Heisel-Sure, M. Y. Kellermann, P. J. Schupp, *Front. Marine Sci.* **2021**, *8*, 665548.
[6] a) Y. S. D. Watkins, J. B. Sallach, *Integr. Environ. Assess. Manage.* **2021**, *17*, 967; b) R. Danovaro, L. Bongiorni, C. Corinaldesi, D. Giovannelli, E. Damiani, P. Astolfi, L. Greci, A. Pusceddu, *Environ. Health Perspect.* **2008**, *116*, 441.
[7] M. M. P. Tsui, H. W. Leung, T.-C. Wai, N. Yamashita, S. Taniyasu, W. Liu, P. K. S. Lam, M. B. Murphy, *Water Res.* **2014**, *67*, 55.
[8] a) Y.-h. Sun, H.-Y. Wu, F.-Q. Xie, J.-R. Ma, Q.-L. Tang, Y.-F. Chen, H. Li, Y.-S. Liu, G.-G. Ying, *Sci. Total Environ.* **2024**, *955*, 176930; b) J. Blasco, C. Trombini, M. Sendra, C. V. M. Araujo, in *Sunscreens in Coastal Ecosystems: Occurrence, Behavior, Effect and Risk*, (Eds: A. Tovar-Sánchez, D. Sánchez-Quiles, J. Blasco), Springer International Publishing, Cham **2020**, pp. 163.
[9] S. L. Schneider, H. W. Lim, *J. Am. Acad. Dermatol.* **2019**, *80*, 266.
[10] D. Vuckovic, A. I. Tinoco, L. Ling, C. Renicke, J. R. Pringle, W. A. Mitch, *Science* **2022**, *376*, 644.
[11] C. A. Downs, M. S. Diaz-Cruz, W. T. White, M. Rice, L. Jim, C. Punihaole, M. Dant, K. Gautam, C. M. Woodley, K. O. Walsh, J. Perry, E. M. Downs, L. Bishop, A. Garg, K. King, T. Paltin, E. B. McKinley, A. I. Beers, S. Anbumani, J. Bagshaw, *J. Hazard. Mater.* **2022**, *438*, 129546.
[12] a) U. Khanna, K. Singh, *J. Eur. Acad. Dermatol. Venereol.* **2023**, *37*, 314; b) A. J. Conway, M. Gonsior, C. Clark, A. Heyes, C. L. Mitchelmore, *Sci. Total Environ.* **2021**, *796*, 148666; c) T. Thomas, M. Fat, G. Kearns, *Front. Marine Sci.* **2024**, *11*, 1471574.
[13] a) A. Siller, S. C. Blaszak, M. Lazar, E. Olasz Harken, *Plast. Aesthetic Nurs.* **2018**, *38*, 158; b) D. Stien, F. Clergeaud, A. M. S. Rodrigues, K. Lebaron, R. Pillot, P. Romans, S. Fagervold, P. Lebaron, *Anal. Chem.* **2019**, *91*, 990.
[14] L. Ouchene, I. V. Litvinov, E. Netchiporouk, *J. Cutaneous Med. Surg.* **2019**, *23*, 648.
[15] J. Tsatalis, B. Burroway, F. Bray, *J. Am. Acad. Dermatol.* **2020**, *82*, 1015.
[16] a) J. L. Espinoza Acosta, E. G. Figueroa Espinoza, M. de la Rosa Alcaraz, *BioResources* **2022**, *17*, 3674; b) M. B. Ariede, W. A. Gomez Junior, T. M. Cândido, M. M. de Aguiar, C. Rosado, C. D. Rangel-Yagui, F. V. Pessoa, M. V. Velasco, A. R. Baby, *Cosmetics* **2024**, *11*, 141.
[17] a) S. Chen, Q. Shi, T. Jang, M. S. B. Ibrahim, J. Deng, G. Ferracci, W. S. Tan, N. J. Cho, J. Song, *Adv. Funct. Mater.* **2021**, *31*, 2106276; b) R. C. Mundargi, M. G. Potroz, S. Park, J. H. Park, H. Shirahama, J. H. Lee, J. Seo, N.-J. Cho, *Adv. Funct. Mater.* **2016**, *26*, 487; c) Z. Zhao, J. Kumar, Y. Hwang, J. Deng, M. S. B. Ibrahim, C. Huang, S. Suresh, N. J. Cho, *Proc. Natl. Acad. Sci. USA* **2021**, *118*, 2113715118; d) J. Deng, Z. Zhao, X. Y. Yeo, C. Yang, J. Yang, A. R. Ferhan, B. Jin, C. Oh, S. Jung, S. Suresh, N. J. Cho, *Adv. Mater.* **2024**, *36*, 2311684.
[18] C. Shi, H. Liu, *Plant Physiol.* **2021**, *187*, 1096.
[19] P. E. Jardine, F. A. J. Abernethy, B. H. Lomax, W. D. Gosling, W. T. Fraser, *Rev. Palaeobot. Palynol.* **2017**, *238*, 1.
[20] a) K. Zdunska, A. Dana, A. Kolodziejczak, H. Rotsztejn, *Skin Pharmacol. Physiol.* **2018**, *31*, 332; b) Y. C. Boo, *Antioxidants (Basel)* **2019**, *8*, 379; c) Y. Wang, Q. Yang, H. Jiang, B. Wang, Y. Bi, Y. Li, D. Prusky, *Postharvest Biol. Technol.* **2020**, *170*, 111325.
[21] F. Liu, H. Peng, J. E. A. Marshall, B. H. Lomax, B. Bomfleur, M. S. Kent, W. T. Fraser, P. E. Jardine, *Sci. Adv.* **2023**, *9*, abc6102.
[22] T. F. Fan, S. Park, Q. Shi, X. Zhang, Q. Liu, Y. Song, H. Chin, M. S. B. Ibrahim, N. Mokrzecka, Y. Yang, H. Li, J. Song, S. Suresh, N. J. Cho, *Nat. Commun.* **2020**, *11*, 1449.
[23] C. Zhou, J. Deng, T. J. Hao, S. Basu, J. Yang, J. Li, C. Yang, Z. Zhao, N. J. Cho, *Annu. Rev. Chem. Biomol. Eng.* **2024**, *15*, 1.
[24] L. Latonen, Y. Taya, M. Laiho, *Oncogene* **2001**, *20*, 6784.
[25] M. Yamada, T. W. Prow, *Adv. Drug Delivery Rev.* **2020**, *153*, 2.

[26] K.-D. A. Theoharis, C. Theoharides, A. Angelidoua, D.-A. Delivanis, N. Sismanopoulosa, B. Zhanga, S. Asadi, M. Vasiadia, Z. Weng, A. Miniati, D. Kalogeromitros, *Bioch. Biophys. Acta* **2012**, *1822*, 21.
[27] E. Rognoni, G. Goss, K. H. S. Toru Hiratsuka, T. Kirk, K. I. Kober, P. P. W. Lui, V. S. K. Tsang, N. J. Hawkshaw, S. M. Pilkington, I. Cho, N. Ali, L. E. Rhodes, F. M. Watt, *eLife* **2021**, *10*, 71052.
[28] a) S. G. Martins, R. Zilhao, S. Thorsteinsdottir, A. R. Carlos, *Front. Genet.* **2021**, *12*, 673002; b) Y. R. Jung, E. K. Lee, D. H. Kim, C. H. Park, M. H. Park, H. O. Jeong, T. Yokozawa, T. Tanaka, D. S. Im, N. D. Kim, B. P. Yu, S. H. Mo, H. Y. Chung, *J. Nat. Prod.* **2015**, *78*, 2110; c) M. M. Bashir, M. R. Sharma, V. P. Werth, *J. Invest. Dermatol.* **2009**, *129*, 994.
[29] R. Raghow, *FASEB J.* **1994**, *8*, 823.
[30] H. Ihn, *Curr. Opin. Rheumatol.* **2002**, *14*, 681.
[31] M. Chvapil, D. P. Speer, J. A. Owen, T. A. Chvapil, *Plast. Reconstr. Surg.* **1984**, *73*, 438.
[32] B. Lin, Y. Zeng, G. P. Asner, D. S. Wilcove, *Nat. Sustainability* **2023**, *6*, 254.
[33] a) V. J. Bykov, J. A. Marcusson, K. Hemminki, *Cancer Res.* **1998**, *58*, 2961; b) P. Autier, J. F. Dore, A. C. Reis, A. Grivegnee, L. Ollivaud, F. Truchetet, E. Chamoun, N. Rotmensz, G. Severi, J. P. Cesarini, *Br. J. Cancer* **2000**, *83*, 1243.
[34] J. D. S. Mansur, M. N. R. Breder, M. C. D. A. Mansur, R. D. Azulay, *An. Bras. Dermatol.* **1986**, *61*, 121.
[35] I. B. Miller, S. Pawlowski, M. Y. Kellermann, M. Petersen-Thiery, M. Moeller, S. Nietzer, P. J. Schupp, *Environ. Sci. Europe* **2021**, *33*, 74.
[36] A. Snyder, M. Valdebran, D. Terrero, K. T. Amber, K. M. Kelly, *Sports Med. Open* **2020**, *6*, 42.
[37] a) S. Santander Ballestín, M. J. Luesma Bartolomé, *Appl. Sci.* **2023**, *13*, 712; b) M. Chatzigianni, P. Pavlou, A. Siamidi, M. Vlachou, A. Varvaresou, S. Papageorgiou, *Ecotoxicology* **2022**, *31*, 1331.
[38] O. B. Hoegh-Guldberg, J. F. Bruno, *Science* **2010**, *328*, 1523.
[39] R. van Woesik, T. Shlesinger, A. G. Grottoli, R. J. Toonen, R. Vega Thurber, M. E. Warner, A. Marie Hulver, L. Chapron, R. H. McLachlan, R. Albright, E. Crandall, T. M. DeCarlo, M. K. Donovan, J. Eirin-Lopez, H. B. Harrison, S. F. Heron, D. Huang, A. Humanes, T. Krueger, J. S. Madin, D. Manzello, L. C. McManus, M. Matz, E. M. Muller, M. Rodriguez-Lanetty, M. Vega-Rodriguez, C. R. Voolstra, J. Zaneveld, *Glob. Chang. Biol.* **2022**, *28*, 4229.
[40] a) Y. Zeng, X. He, Z. Ma, Y. Gou, Y. Wei, S. Pan, L. Tao, *Cell Rep. Phys. Sci.* **2023**, *4*, 101308; b) T. He, M. M. P. Tsui, C. J. Tan, C. Y. Ma, S. K. F. Yiu, L. H. Wang, T. H. Chen, T. Y. Fan, P. K. S. Lam, M. B. Murphy, *Environ. Pollut.* **2019**, *245*, 462.
[41] a) H. Malektaj, A. D. Drozdov, J. deClaville Christiansen, *Polymers* **2023**, *15*, 3012; b) C. Croitoru, M. A. Pop, T. Bedo, M. Cosnita, I. C. Roata, I. Hulka, *Polymers* **2020**, *12*, 560.
[42] N.-J. Cho, *Mater. Today* **2022**, *61*, 1.